

## Experimental Advances for High-Speed Evaluation of Electron Densities

Peter Luger,<sup>\*,†</sup> Armin Wagner,<sup>‡</sup> Christian B. Hübschle,<sup>†</sup> and Sergey I. Troyanov<sup>§</sup>

*Freie Universität Berlin, Institut für Chemie/Kristallographie, Takustr. 6, 14195 Berlin, Germany, Swiss Light Source (SLS) at the Paul-Scherrer Institute, Villigen, Switzerland, and Chemistry Department, Moscow State University, Russia*

*Received: June 28, 2005; In Final Form: October 10, 2005*

Evaluating electron densities of entire classes of chemically or biologically related compounds is within reach thanks to advances in high-speed high-resolution synchrotron diffraction: a 12 h sequence of diffraction experiments has been conducted at the beamline X10SA of the Swiss Light Source (SLS). It resulted in four high-resolution X-ray data sets used for experimental electron density determinations of the two halogenated fullerenes C<sub>60</sub>F<sub>18</sub> and C<sub>60</sub>Cl<sub>30</sub>, the Watson and Crick base pair adenine-thymine and the tripeptide L-Ala-Gly-L-Ala. Application is considered relevant for life sciences where the study of structure-guided biological recognition processes can now be completed by electronic information of entire series of molecules.

Thanks to technical advances in the past decade, high throughput techniques were established in various fields of X-ray diffraction-based structure research. The use of highly intense beamlines of third generation synchrotrons and the introduction of large area detectors in combination with highly automated experimental and computational procedures have made high-speed structure information available not only from powder diffraction or small molecule structure analysis but also in protein crystallography, where usually extensive X-ray diffraction experiments have to be performed. One field of X-ray-based structure research where high throughput techniques are not yet available is experimental electron density work.<sup>1</sup> In contrast to protein crystallographic experiments, X-ray data have to be collected at high resolution ( $d < 0.5 \text{ \AA}$ ), making more flexible experimental setups necessary.

The importance of the electron density  $\rho(\mathbf{r})$  as a fundamental property of an electronic system is highlighted by the Hohenberg–Kohn theorem.<sup>2</sup> It states that the ground-state energy of a nondegenerate quantum chemical system is functionally related to its distribution of charge. Hence, major electronic properties, such as quantitative information about atomic and bond properties,<sup>3</sup> nonbonding interactions, stability, and reactivity can be deduced from the electron density.

In medicinal chemistry, where it is a fundamental challenge to understand drug–target recognition processes, the knowledge of the electronic charge density is a valuable completion of structure information and serves as a basis for a better understanding of such interactions than the consideration of steric properties only. Since rapid screening of a large number of chemical compounds is indispensable in structure-guided drug discovery, the generation of electronic information of series of molecules at an increased pace would be highly desirable.

Some time ago, we reported on an X-ray diffraction experiment that combined high-intensity synchrotron primary radiation and CCD area detection.<sup>4</sup> This experiment was considered a first step to expedite the electron density diffraction experiment which otherwise took weeks or even months.

Here, we report on a 12 h sequence of synchrotron diffraction experiments which resulted in four high-resolution data sets for experimental electron density work. Although the experiments detailed below were in certain parts of a preliminary stage, we believe that they also open high throughput techniques to enter this field.

The experiments were carried out at the protein crystallography beamline X10SA of the Swiss Light Source (SLS) at Paul Scherrer Institute (Villigen, Switzerland). Diffraction data were collected at 92 K with a MAR225 CCD area detector at a wavelength of  $\lambda = 0.6214 \text{ \AA}$  (focus size  $50 \times 10 \mu\text{m}^2$ ,  $h \times v$ , fwhm). Variable detector positions and an arc (4DX-ray Systems AB) mounted on the goniometer head allowed us to overcome the limitations from the single-axis geometry and to improve the completeness of data in the high-resolution region. The diffracted intensities cover a range of several orders of magnitude, which cannot be resolved by CCD detectors. Therefore, the primary beam had to be attenuated down to less than 1% for certain detector positions.

As the summary of data collections shows (Table 1), it was possible to measure a total of  $\sim 440\,000$  reflections in a 12 h period for four crystals of different compounds at a resolution of generally  $d = 0.5 \text{ \AA}$  ( $\sin \theta/\lambda = 1.0 \text{ \AA}^{-1}$ ).

In all cases, significant intensities could be obtained even in the very high angle regions of reciprocal space. One particular example is the data collection of the C<sub>60</sub>F<sub>18</sub> crystal, which was the smallest of the crystals used with tiny dimensions in two directions. Nevertheless, the outer regions were densely populated with significant intensities as the mean  $I/\sigma(I)$  ratio of 41.0 in the highest-resolution shell shows (see Table 1).

\* Corresponding author. E-mail: luger@chemie.fu-berlin.de.

<sup>†</sup> Freie Universität Berlin.

<sup>‡</sup> Swiss Light Source (SLS) at the Paul-Scherrer Institute.

<sup>§</sup> Moscow State University.

**TABLE 1: Summary of Data Collections at Beamline X10SA of the SLS**

compound <sup>a</sup>	C <sub>60</sub> F <sub>18</sub> (i)	C <sub>60</sub> Cl <sub>30</sub> (ii)	MAMT (iii)	AGA (iv)
space group	<i>Cc</i>	<i>P2<sub>1</sub>/n</i>	<i>P2<sub>1</sub>/m</i>	<i>P2<sub>1</sub></i>
cell volume [Å <sup>3</sup> ]	3593.8	2863.3	668.4	577.1
crystal size [mm <sup>3</sup> ]	1.0 × 0.1 × 0.06	0.3 × 0.2 × 0.1	0.3 × 0.3 × 0.14	0.5 × 0.2 × 0.18
total no. of reflections	216 676	139 741	46 824	33 733
unique	28 053	22 950	5682	4662
<i>R</i> <sub>int</sub> <sup>b</sup>	0.041 (0.044)	0.040 (0.067)	0.044 (0.055)	0.038 (0.055)
mean <i>I</i> / $\sigma$ ( <i>I</i> ) <sup>b</sup>	56.2 (41.0)	32.5 (17.8)	32.5 (22.5)	26.0 (18.4)
completeness [%] <sup>b</sup>	93.0 (87.1)	95.7 (91.0)	98.4 (98.9)	82.3 (71.0)
redundancy	7.7	6.1	8.2	7.2
<i>R</i> <sub>1</sub> (spherical)	0.046	0.043	0.031	0.040
<i>R</i> <sub>1</sub> (multipol)	0.034	0.024	0.022	0.026

<sup>a</sup> The compounds investigated were (i) fluorinated C<sub>60</sub>-fullerene C<sub>60</sub>F<sub>18</sub>,<sup>13</sup> (ii) chlorinated C<sub>60</sub>-fullerene C<sub>60</sub>Cl<sub>30</sub>,<sup>14</sup> (iii) MAMT: the base pair 9-methyladenine-1-methylthymine,<sup>15</sup> (iv) AGA: the tripeptide L-alanyl-glycyl-L-alanine.<sup>16</sup> <sup>b</sup> The values in parentheses are for the highest resolution shell 0.5–0.6 Å.

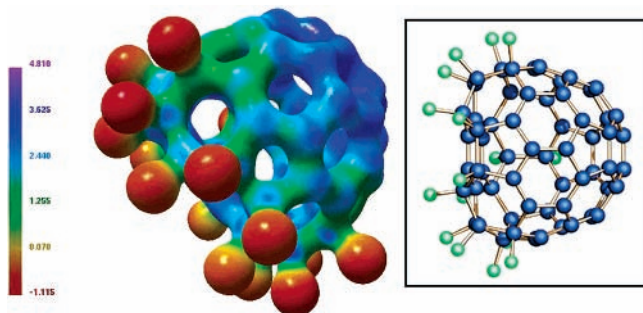


**Figure 1.** Left: Experimental electrostatic potential (EP) of C<sub>60</sub>F<sub>18</sub> mapped on the electron density isosurface at  $\rho = 0.8 \text{ e}/\text{\AA}^3$ . The color code (see color bar) illustrates negative EP distributions (dark red) in the region of the fluorine substituents; the positive regions (dark blue) cover the opposite non-halogenated C<sub>60</sub> surface. Illustration generated with the in-house-written program MOLISO.<sup>17</sup> Right: Molecular structure of C<sub>60</sub>F<sub>18</sub>. In contrast to the spherical shape of the free C<sub>60</sub> fullerene, the C<sub>60</sub>F<sub>18</sub> molecule is heavily deformed toward a half-sphere due to the fluorine substitution.<sup>13</sup>

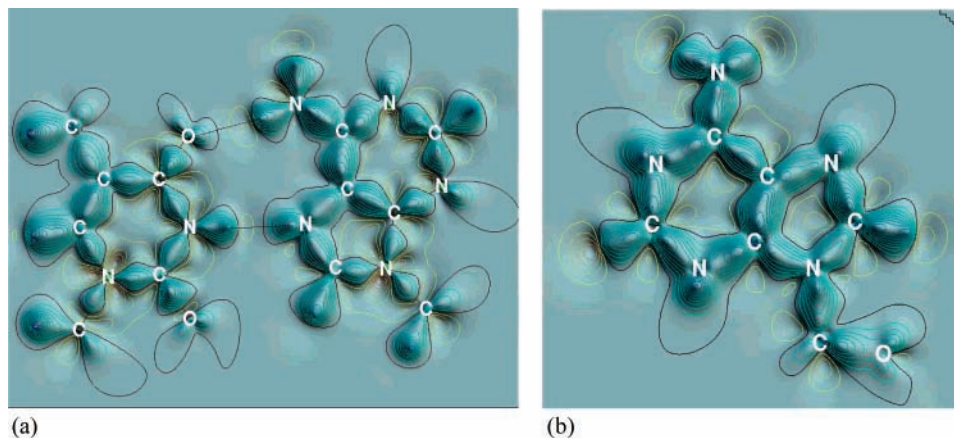
Although not all data sets are finally processed and refined, some preliminary electron density results can be presented. These were obtained by application of the Hansen and Coppens aspherical-atom model<sup>5</sup> as implemented in the computer program package XD.<sup>6</sup> Figure 1 shows the electrostatic potential of C<sub>60</sub>F<sub>18</sub> calculated from the experimental data using the method of Su and Coppens.<sup>7</sup> An extended electronegative region is seen around the fluorine substituents, while the opposite non-fluorinated carbon surface is positive.

Figure 2a shows a static deformation density distribution in the plane of the Watson and Crick base pair complex 9-methyladenine-1-methylthymine which was obtained by subtraction

of a spherical promolecular density from the total experimental electron density. Charge accumulation is seen on all covalent bonds. In the hydrogen bond regions (see dotted lines in Figure 2a), which are of certain interest in this complex, oxygen and nitrogen lone-pair electron densities show some charge rearrangement due to the N–H···N and N–H···O interactions.

In addition to the four data sets listed in Table 1, a quick test data set was measured for an adenosine crystal which took less than 1 h. More than 22 000 reflections were collected, which were nicely suited for a further aspherical atom refinement. Figure 2b shows the static map in the purine plane of the adenosine molecule where the covalent bonding features are again properly resolved, although the data set of this compound was subject of one of the shortest measurements ever carried out in experimental charge density work.

The data sets summarized in Table 1 show some limitations, which are all related to the typical experimental setup for a protein crystallography beamline. These are mostly of mechanical and hence geometric nature and could be overcome with little effort. The most important parameter to be improved is the resolution. Because of the brilliant primary intensity, all samples diffracted better than  $d = 0.5 \text{ \AA}$ , the limit given by the diffractometer geometry. The *I*/ $\sigma$ (*I*) ratio of typically  $> 15$  in the highest-resolution shell indicates that even for otherwise weakly diffracting crystals the resolution limit can be extended to 0.3–0.4 Å, which can hardly be reached with a sealed tube or a rotating anode. This is highly desirable for experimental charge density work and could be easily achieved by minor mechanical changes at the diffractometer setup or by making use of a shorter wavelength. The overall data set quality and completeness, which should be increased, are also related to



**Figure 2.** Relief plots of the experimental static deformation densities of the Watson and Crick base pair 9-methyladenine-1-methylthymine (a) and of the purine plane of adenosine (b).

minor mechanical amendments and are not principal problems. Finally, the data collection temperature can be reduced to  $\sim 10$  K. First tests with a He open-flow low-temperature device at the beamline have been proven successful.

To get an estimate about the quality of the short duration experiments at the SLS and the influences of the present limitations mentioned above, we compare the results of the AGA data set with a second highly resolved state-of-the-art data set measured at beamline D3 of the Hasylab/DESY Hamburg. This second data collection of AGA took 28 h to give 97 469 reflections, 9406 unique, up to  $d = 0.4 \text{ \AA}$  ( $\sin \theta/\lambda = 1.25 \text{ \AA}^{-1}$ ). Refinement with exactly the same multipole model as for the SLS data gave very comparable residuals and bond topological properties (for details, see Supporting Information) which are not significantly different from the SLS data. For the 14 non-H-bonds, the electron density ( $\rho_{\text{bcp}}$ ) and Laplacian values ( $\nabla^2 \rho_{\text{bcp}}$ ) at the bond critical points (bcp's) were compared, and average differences were found to be  $0.11(5) \text{ e \AA}^{-3}$  and  $4.0(21) \text{ e \AA}^{-5}$  for  $\rho_{\text{bcp}}$  and  $\nabla^2 \rho_{\text{bcp}}$ , respectively. This is exactly the range given by several authors<sup>8–10</sup> to be considered if electron density results from different experiments are compared. Supported by these quantitative findings, our 12 h experimental sequence has demonstrated that high throughput techniques are now within reach for experimental electron density work to yield quantitative results of the current standard. Moreover, the example of the  $\text{C}_{60}\text{F}_{18}$  experiment has proven that high-resolution data can be collected even for tiny crystals with the extra advantage of practically absorption- and extinction-free data. Application of the recently introduced invariom model<sup>11,12</sup> that makes use of transferable pseudo atoms from a database and provides tools for an almost automatic assignment of the multipole model could further speed up the refinement procedure of the experimental data, so that electron density determination within minutes can be expected soon. Evaluating electron densities of entire classes of chemically or pharmacologically related compounds can therefore become a routine task to be carried out in time periods comparable to the ones currently needed for conventional X-ray analyses.

**Acknowledgment.** Funded by the Deutsche Forschungsgemeinschaft within the priority program SPP 1178 and grants

Lu 222/24-3, Lu 222/27-1, and the NCCR for Structural Biology. We thank E. Pohl, C. Pradervand, E. Zimoch, and R. Schneider for their help to set up the detector rotation. Mrs. D. Förster kindly provided the Supporting Information material.

**Supporting Information Available:** Topological properties and an accompanying figure. This material is available free of charge via the Internet at <http://pubs.acs.org>.

## References and Notes

- (1) Coppens, P. *X-ray Charge Densities and Chemical Bonding*; Oxford University Press: New York, 1997.
- (2) Hohenberg, P.; Kohn, W. *Phys. Rev.* **1964**, *136*, B864–B871.
- (3) Bader, R. F. W. *Atoms in Molecules, A Quantum Theory*; Clarendon: Oxford, 1990. Bader, R. F. W.; Lode, P.; Popelier, A.; Keith, T. A. *Angew. Chem., Int. Ed. Engl.* **1994**, *33*, 620–631.
- (4) Koritsanszky, T.; Flaig, R.; Zobel, D.; Krane, H.-G.; Morgenroth, W.; Luger, P. *Science* **1998**, *279*, 356–358.
- (5) Hansen, N. K.; Coppens, P. *Acta Crystallogr., Sect. A* **1978**, *34*, 909–921.
- (6) Koritsanszky, T.; Richter, T.; Macchi, P.; Volkov, A.; Gatti, C.; Howard, S.; Mallinson, P. R.; Farrugia, L.; Su, Z. W.; Hansen, N. K. XD, A Computer Program Package for Multipole Refinement and Analysis of Electron Densities from Diffraction Data; Freie Universität Berlin, 2003.
- (7) Su, Z.; Coppens, P. *Acta Crystallogr., Sect. A* **1992**, *48*, 188–197.
- (8) Pichon-Pesme, V.; Lachekar, H.; Souhasson, M.; Lecomte, C. *Acta Crystallogr. Sect. B* **2000**, *56*, 728–737.
- (9) Dittrich, B.; Koritsanszky, T.; Grosche, M.; Scherer, W.; Flaig, R.; Wagner, A.; Krane, H. G.; Kessler, H.; Riemer, C.; Schreurs, A. M. M.; Luger, P. *Acta Crystallogr., Sect. B* **2002**, *58*, 721–727.
- (10) Messerschmidt, M.; Scheins, S.; Luger, P. *Acta Crystallogr., Sect. B* **2005**, *61*, 115–121.
- (11) Dittrich, B.; Koritsanszky, T.; Luger, P. *Angew. Chem., Int. Ed.* **2004**, *43*, 2718–2721.
- (12) Dittrich, B.; Hübschle, C. B.; Messerschmidt, M.; Kalinowski, R.; Gint, D.; Luger, P. *Acta Crystallogr., Sect. A* **2005**, *61*, 314–320.
- (13) Goldt, I. V.; Boltalina, O. V.; Sidorov, L. N.; Kemnitz, E.; Troyanov, S. I. *Solid State Sci.* **2002**, *4*, 1395–1401.
- (14) Troshin, P. A.; Lyuboskaya, R. N.; Ioffe, I. N.; Shustova, N. B.; Kemnitz, E.; Troyanov, S. I. *Angew. Chem., Int. Ed.* **2004**, *44*, 234–237.
- (15) Hoogsteen, K. *Acta Crystallogr., Sect. A* **1963**, *16*, 907–916. Fray, M. N.; Koetzle, T. F.; Lehmann, M. S.; Hamilton, W. C. *J. Chem. Phys.* **1973**, *59*, 915–924.
- (16) Förster, D.; Messerschmidt, M.; Luger, P. *Acta Crystallogr., Sect. C* **2005**, *61*, o420–o421.
- (17) Hübschle, C. B. MOLISO, a program for the visualization of the electrostatic potential; Free University Berlin, 2005.